System Identification Experiments on a Large-Scale Unmanned Helicopter for Autonomous Flight

Seiji Hashimoto*[1], Tomonori Ogawa*, Shuichi Adachi*[2] Anzhong Tan**[1] and Gou Miyamori**[2]

*Dept. of Electrical and Electronic Eng.
Utsunomiya University
7-1-2 Yoto, Utsunomiya
Tochigi 321-8585 JAPAN
Phone +81-28-689-6125, Fax +81-28-689-6125
E-mail: *[1] hashimoto@ieee.org
*[2] adachis@cc.utsunomiya-u.ac.jp

**Kawada Industries, Inc.
122-1 Hagadai, Haga-machi, Haga-gun
Tochigi 321-3325 JAPAN

Phone +81-28-677-5737, Fax +81-28-677-5707
E-mail: **[1] anzhong.tan@kawada.co.jp
**[2] go.miyamori@kawada.co.jp

Abstract— **Unmanned helicopters are now used to spray agricultural chemicals and are also used to take aerial photographs. In addition, the aircrafts are expected for wide activities such as watching and rescuing in near future. Then, an autonomous flight using several sensors typified by GPS is expected.**

In this paper, system identification experiments have been carried out for a large-scale unmanned helicopter. Using the input and output data, system identification results on the dynamics are shown through numerical analysis. Moreover, the effectiveness of the identified model is demonstrated through a position control based on the $\mathcal{H}_\infty$ theory.

Keywords— **unmanned helicopter, system identification, autonomous flight**

I. Introduction

Recently, an unmanned helicopter, particularly a large-scale one, is expected not only for the fields such as agricultural spraying and taking aerial photographs, but also for the fields such as watching, rescuing, fire fighting, and so on. For these monotonous or dangerous missions, an autonomous flight control of the helicopter is indispensable. The autonomous flight control requires synthesizing technologies such as trouble diagnosis and dangerous object avoidance as well as attitude and position controls.

The flight control of the helicopter is difficult due to the following;

(1) The dynamics of the helicopter is essentially unstable.
(2) There are nonlinear variations in dynamics with air speed.
(3) The helicopter has six degrees of freedom in its motions (up/down, fore/aft, right/left, rolling, pitching, yawing).
(4) The helicopter is a multi-input multi-output (MIMO) system.
(5) Flight modes are cross-coupled.
(6) The flight is easily affected by disturbances such as wind, temperature, etc.

The helicopter, however, can be modeled as a linear system around trim points, i.e., a flight with no accelerations and no moments. Moreover, the system can be stabilized by using a stability augmentation system (SAS), which can also reduce the influence of cross-couple terms. Therefore, the flight control of the unmanned helicopter with SAS is possible around the trim points. Several unmanned helicopters have been developed[1],[2], or are under development throughout the world. However, a complete autonomous flight control system has not been realized.

The goal of our research is an autonomous flight control of a large-scale unmanned helicopter. The authors, at first, experimented on system identification of the full-scale unmanned helicopter (named RoboCopter) to derive the mathematical model of the helicopter. Using the measured input and output data, the dynamics of the helicopter is identified, and then numerically illustrated the applicability of the identified models to the position control for the autonomous flight.

II. Large-Scale Unmanned Helicopter

The configuration of an autonomous flight control of a large-scale unmanned helicopter is shown in Fig. 1. The flight control of the body is accomplished by using various sensors, which are represented by a global positioning system (GPS), in accordance with the command reference transmitted by the ground station. The signals that lack for the autonomous flight can be esti-

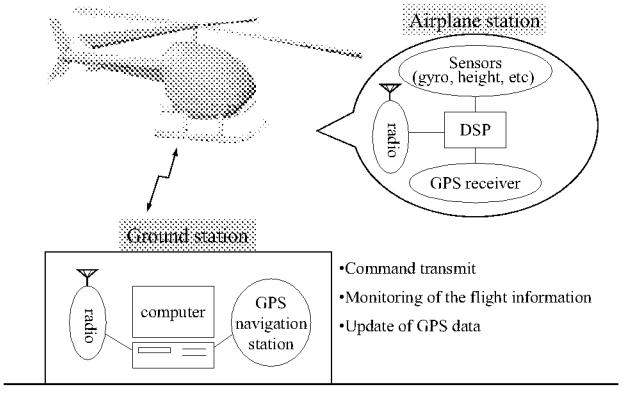

Fig. 1. Configuration of an autonomous flight system.

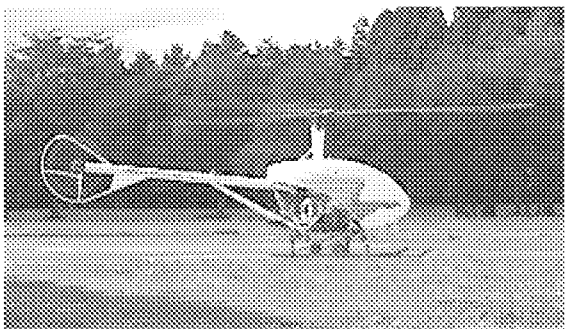

Fig. 2. The experimental large-scale unmanned helicopter (RoboCopter).

TABLE I
TYPICAL PARAMETERS OF ROBOCOPTER

body dimensions	length	7.31[m]
	width	1.99[m]
	height	2.65[m]
weight	total weight	794[kg]
	empty weight	500[kg]
	payload	294[kg]
engine	type	air-cooled 4-cycle engine
	power	124[kW](168HP)
main rotor	number of blade	3
	diameter	8.18[m]
tail rotor	number of blade	2
	diameter	1.30[m]
continuous flight time		100[min](extendable to 4[h] depending on payload)

mated by the on-board digital signal processor (DSP). The control algorithm for the flight is also installed in DSP in advance. Thus the unmanned helicopter can be remotely controlled from the ground. For this experiment, it is designed that a remote operator can transmit a rudder modification signal directly to the flight control in order to keep the flight safe.

The full-scale unmanned helicopter (RoboCopter), which is developed by Kawada Industries, Inc.[3], is shown in Fig.2. The parameters of the helicopter are shown in Table I. This unmanned helicopter is a remodeled version of a manned helicopter. The flight time can be extended from 100 min to 240 min at the cost of payload. In addition, stability of the helicopter is improved by the stability augmentation system (SAS) installed in DSP.

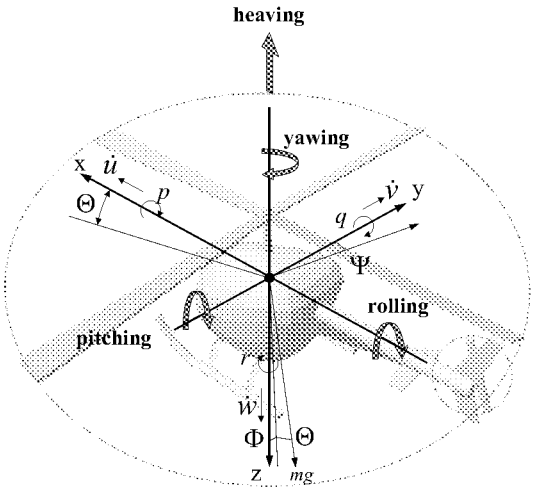

Fig. 3. Helicopter coordinates.

III. EXPERIMENTS ON SYSTEM IDENTIFICATION OF HELICOPTER DYNAMICS

A. Nomenclature

Fig.3 shows the coordinates to describe the motion of the helicopter. The origin of helicopter axes is placed on the center of gravity. The variables, constants and terms in the figure are defined as follows;

x, y, z :	aircraft fixed coordinates
p, q, r :	angular velocities around x, y, z-axes, respectively
x, y, z :	positions in x, y, z directions, respectively
u, v, w :	velocities in x, y, z directions, respectively
Φ, Θ, Ψ :	roll, pitch, yaw angles, respectively
θ_C :	lateral cyclic pitch angle
θ_S :	longitudinal cyclic pitch angle
θ_{0T} :	tail rotor pitch angle
θ_{0M} :	main rotor collective pitch angle
m :	mass of helicopter
g :	gravitational acceleration

rolling :	A rotational motion around the x-axis of the body which occurs by changing θ_C
pitching :	A rotational motion around the y-axis of the body which occurs by changing θ_S
yawing :	A rotational motion around the z-axis of the body which occurs by changing θ_{0T}
heaving :	A linear motion in the z-axis direction of the body which occurs by changing θ_{0M}

Each motion is not independent of θ_C, θ_S, θ_{0T}, *and* θ_{0M}, so there exists a cross coupling. One control input to an objective motion causes other different kinds of motion. For example, the heaving motion is coupled to the yawing motion[1].

B. System Identification Experiments

The block diagram of the helicopter compensated

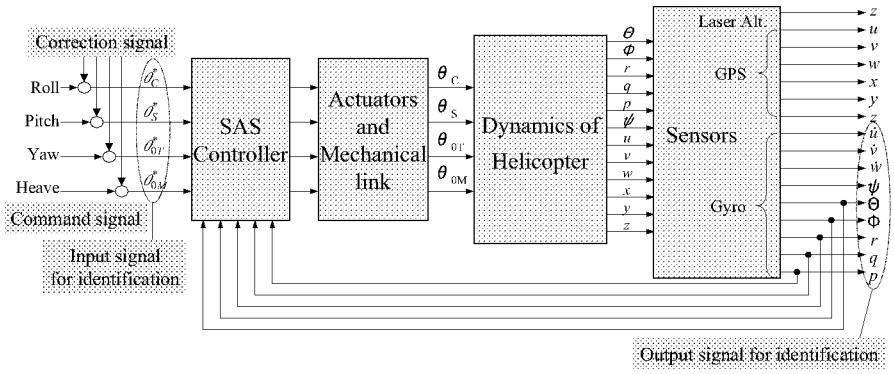

Fig. 4. Construction for system identification experiments on the helicopter with SAS.

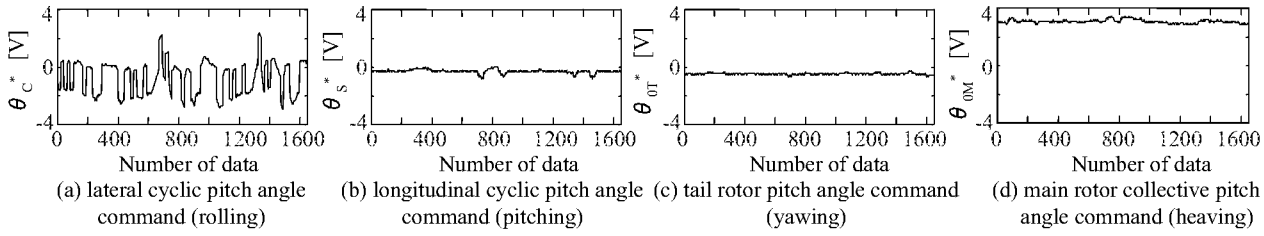

Fig. 5. Input signals (rolling).

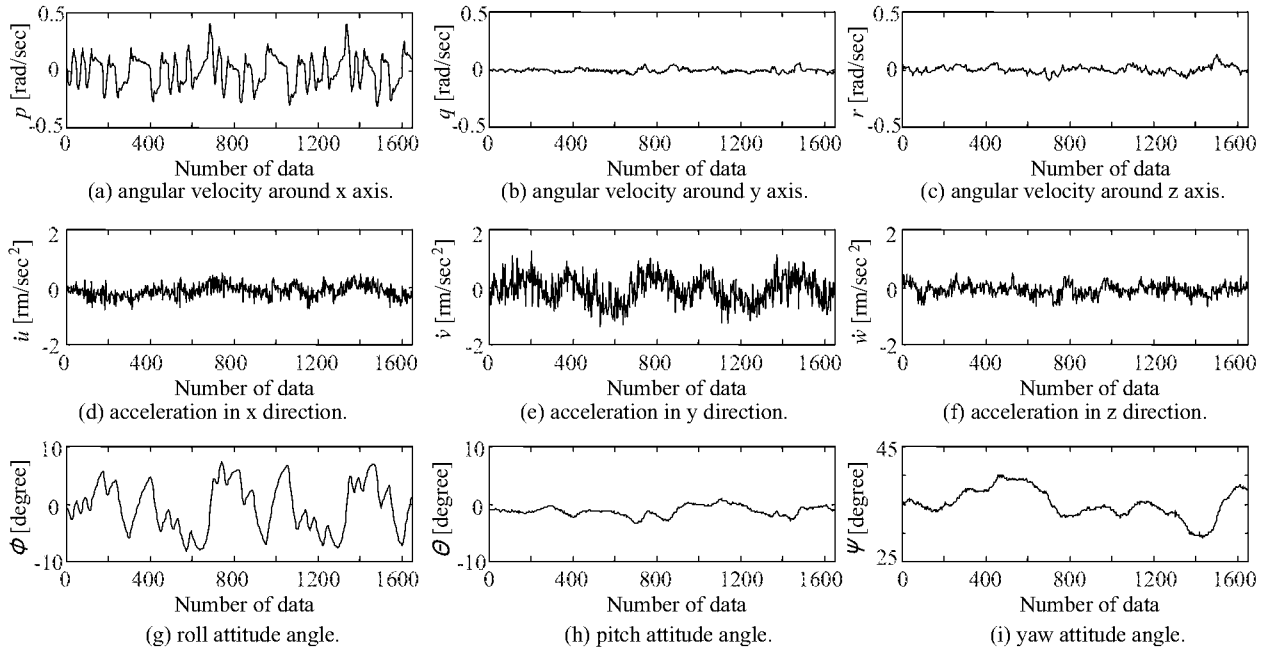

Fig. 6. Output signals (rolling).

by the SAS for system identification is shown in Fig.4. The command references, which are made in the computer on the ground station, are transmitted to the helicopter. Modification rudder signals from the remote operator are added to these command reference, and inputted to the SAS controller for the attitude control. These input signals $\theta_C^*, \theta_S^*, \theta_{0T}^*$ and θ_{0M}^* drive rolling, pitching, yawing and heaving motions, respectively. The superscript * represents the reference value of those signals. $\theta_C^*, \theta_S^*, \theta_{0T}^*$ and θ_{0M}^* were used as input signals for system identification. In this case, taking the cross-couplings into consideration, the each motion was separately excited by the signals. The pseudo random binary signal (PRBS) was applied to the motion, which wants to be identified, and the constant signals were applied to the other three motions. The sampling time for the experiment was 0.02 sec, and the clock period of the input was 20 times of the sampling time. The period of the PRBS was 31. The measured outputs were attitude angles Φ, Θ, Ψ, their angular velocities p, q, r and accelerations $\dot{u}, \dot{v}, \dot{w}$ by an inertial measurement equipment, velocities u, v, w and positions x, y, z by GPS,

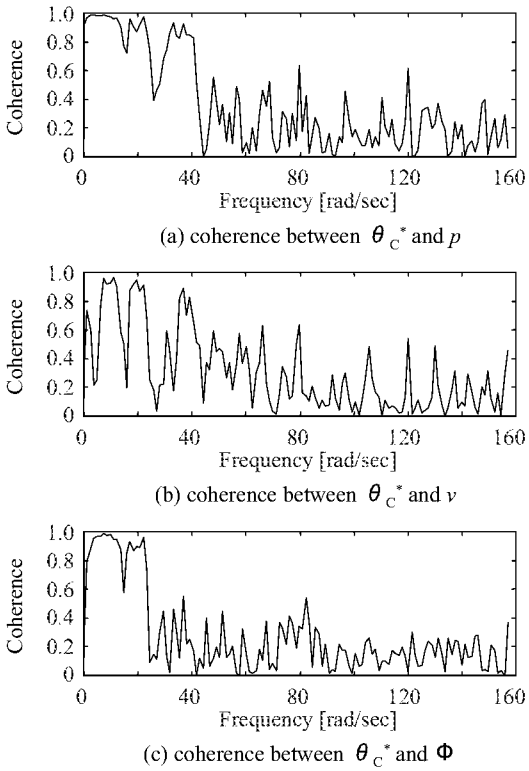

Fig. 7. Coherences for roll excitation.

and height z by a laser height meter. The signals $p, q, r, \dot{u}, \dot{v}, \dot{w}, \Phi, \Theta$ and Ψ which directly influence the control design for the autonomous flight were selected as output signals for system identification.

As an example, a motion about rolling excitation is described below. The measured input and output signals are shown in Figs.5 and 6, respectively. As for the influence to the input signals by the modification rudder signals, it can be confirmed that $\theta_S^*, \theta_{0T}^*$ and θ_{0M}^* are nearly constant values. As is seen in Fig.6, it is verified that the output signals $p, \dot{v}$ and Θ, which are strongly related to a rolling motion, are excited by θ_C^*. Moreover, it is noticed that the couplings mentioned in the earlier chapter are to some extent compensated by SAS. The coherences between the input θ_S^* and the outputs $p, \dot{v}$ and Θ are shown in Fig.7. The accurate identification can be expected at low frequency range because of the high gain of the coherences.

IV. System Identification

Using measured input-output data, system identification is, at first, applied to the helicopter as a single-input single-output (SISO) system, and then applied as a multi-input multi-output (MIMO) system.

A. SISO Identification

In this section, the system identification based on the prediction error method is applied to the helicopter as an SISO system. The number of data was 1650. ARX, ARMAX, OE and BJ models were used to identify the dynamics of the helicopter. The cross-validation

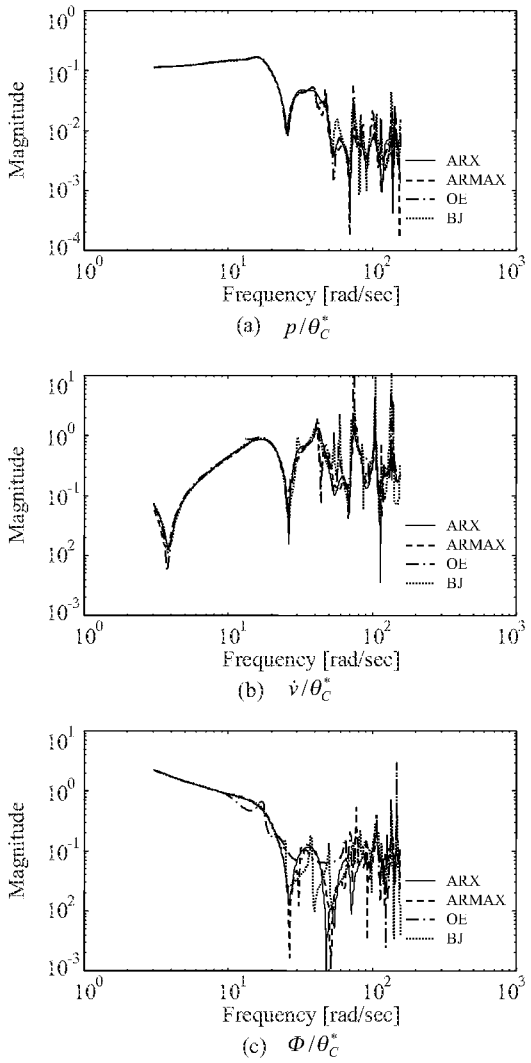

Fig. 8. Gain plots for roll excitation.

was utilized to determine the order of ARX model, and then applied the order for the other models as well. Two third of the data were used for the identification, and the rest data for validation. The model order which can make a least loss function was 30th with two delays.

Fig.8 shows gain plots from θ_C^* to $p, \dot{v}$ and Φ for the rolling motion. As is seen in Fig.8, the deviation among these four gain plots is small enough at the frequency range less than 20 rad/sec, which falls in the range of a position control. Therefore, the frequency responses of the rolling motion can be identified with high accuracy at that frequency range. It is also understood that the rigid body dynamics are dominant at that frequency.

Next, to evaluate the identified model in time domain, the remaining one third input data is applied to the identified ARX model. Fig.9 shows time responses of the model output and the measured output. From Fig.9, it is confirmed that the model output coincides well with the measured output. Therefore, the identified model well describes the rolling motion of the experimental helicopter.

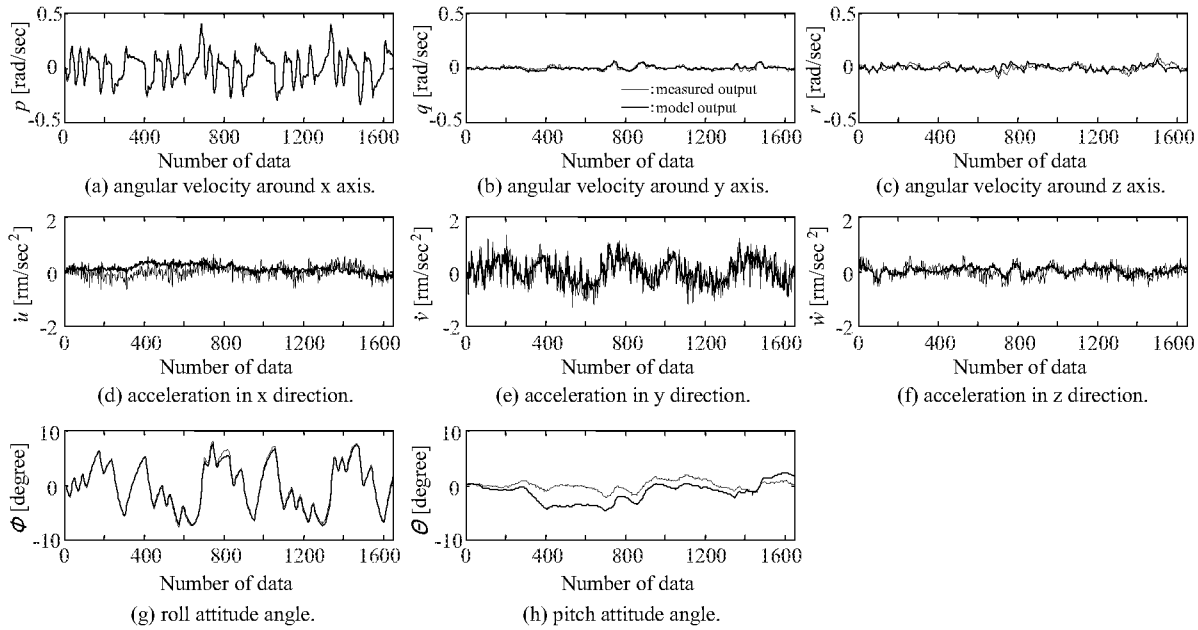

Fig. 10. Comparison of time responses between MIMO identified model output and measured output.

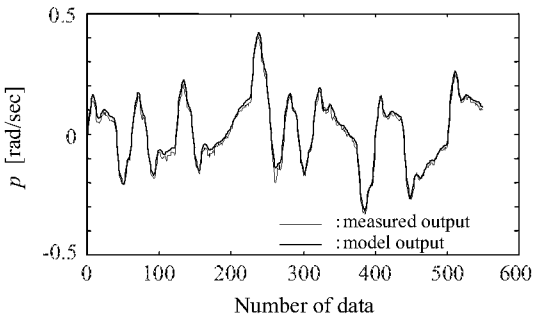

Fig. 9. Time response of ARX model to roll excitation.

B. MIMO Identification

Next, the system identification is applied to the helicopter as an MIMO system for the rolling data. The subspace-based method[4] is utilized for the identification. This is the method which can identify a system as a state-space model, i.e., the MIMO system. Input signals are $\theta_C^*, \theta_S^*, \theta_{0T}^*, \theta_{0M}^*$, and output signals are $p, q, r, \dot{u}, \dot{v}, \dot{w}, \Phi, \Theta$ in which Ψ is excepted for the reason of the stability. The number of data was 1650, and the 31st-order model was used. Fig.10 shows the time responses of the measured outputs and the model outputs to the input signals used in the experiment. In spite of the data of rolling excitation, it is understood that a comparatively good result is obtained for the responses $q, r, \dot{u}, \dot{w}$ that do not correspond to the motions of rolling.

V. A Design Example of Position Control System for Autonomous Flight

In this section, we will illustrate how to use the identified model by means of an example concerning a position control for an autonomous flight. The controller concerning a lateral (right/left) movement of the helicopter is designed based on the $\mathcal{H}_\infty$ control theory[5].

We first consider the dynamics of the rolling motion. The following relations are found with respect to a dynamic balance;

$$m\ddot{y} = F\sin\Phi \quad (1)$$

$$mg = F\cos\Phi \quad (2)$$

where F is the lift. From eqs.(1) and (2), if Φ is small enough, then the relation

$$\ddot{y} = g\Phi \quad (3)$$

is obtained, which implies that y obeys the double integral of Φ to make the lateral movement. Therefore, the double integral of the identified model $\Phi/(\theta_C^* s^2)$ times g, that is, $\Phi/\theta_C^* \cdot g/s^2$, can be considered as the plant for the movement. In this case, it is supposed that the model using the identified 30th-order model(Φ/θ_C^*) shown in Fig.8(c) as the real plant P, and the model using identified 4th-order model as a nominal plant P_n. Fig.11 shows the gain plots of P and P_n. Then, the multiplicative uncertainty Δ_m, which is derived from $\Delta_m = (P - P_n)/P_n$, is shown in Fig.12. It is understood that the limitation of the bandwidth for the position control is less than 20 rad/sec because of its zero-cross frequency. Taking this into consideration, the weighting function W_T, which is for the complementary sensitivity function T, is selected to satisfy the restriction $|\Delta_m| < |W_2(j\omega)|, \forall\omega$, as

$$W_T(s) = \frac{(s/0.25+1)^3}{1000} \quad (4)$$

The gain plot is also shown in Fig.12. In this figure, the bandwidth is selected at 2.5 rad/sec.

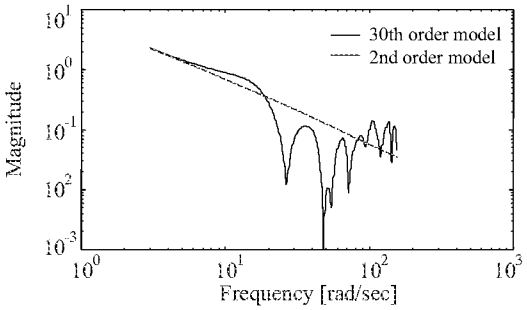

Fig. 11. Gain plots of P and P_n.

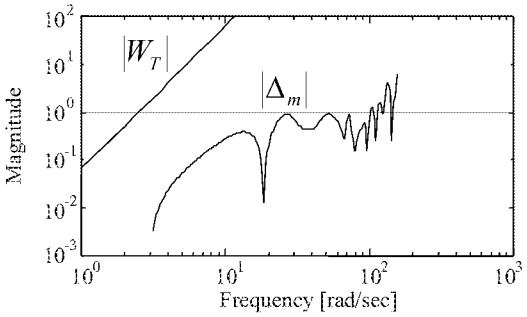

Fig. 12. Gain plots of Δ_m and W_T.

According to the weighting function W_S, which is for the sensitivity function S, it is recommended to be the first order like an integrator as the following, since its dynamics are directly reflected in the $\mathcal{H}_\infty$ controller.

$$W_S(s) = \frac{2.4}{s} \tag{5}$$

The generalized plant including these weighting functions is illustrated in Fig.13. As a result of these weighting functions, the $\mathcal{H}_\infty$ controller of the 4th-order can be obtained as

$$\frac{2.41 \times 10^5 s(s+0.547)(s+55.8)}{(s+74.4)(s+1720)(s^2+2\cdot 0.729\cdot 7.18s+7.18^2)} \tag{6}$$

In order to examine the robust stability of the system, we apply a ramp position reference to the rightward to the system in which the order of the plants is both 4th and 32nd. Fig.14 shows the time responses of the position y, the velocity v and the angle Φ. From the figure, it can be understood that the robust control can be performed by the $\mathcal{H}_\infty$ controller not only to stabilize

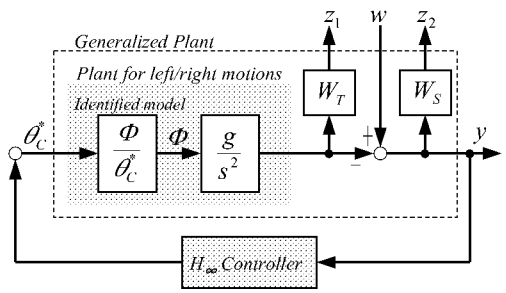

Fig. 13. Generalized Plant.

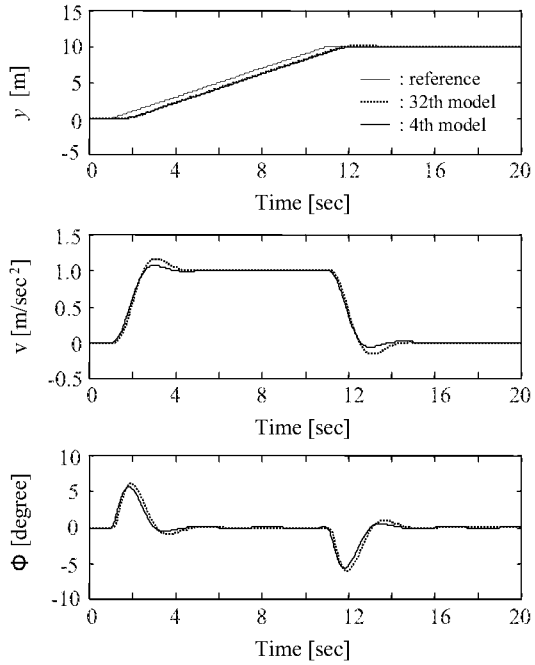

Fig. 14. Time responses to ramp position reference.

the system but also to follow the reference without a steady state error.

VI. Conclusion

System identification experiments were applied to the large-scale unmanned helicopter which was compensated by SAS. The four motions were separately excited, and as an example the dynamics for the rolling motion have been identified both as an SISO system and as an MIMO system based on the measured data.

We also have illustrated how to use the identified model by means of an example concerning a position control, and demonstrated the applicability of the identified model for an autonomous flight.

References

[1] H. T. Nguyen and N. R. Prasad, "Fuzzy Modeling and Control -Selected Works of M. Sugeno," Chapter 2, CRC Press, 1999.

[2] Y. Kobayashi and K. Liu, "Modeling and Robust Control of A Single-Rotor Helicopter," *Proc. of SICE 26th Control Theory Symposium*, pp. 111-116, 1997(in Japanese).

[3] G. Miyamori, Q. Zhao, M. Nakamura, A. Tan, K. Akachi and M. Hirai, "Development of An Unmanned Multipurpose Utility Helicopter(RoboCopter)," *Proc. of 35th Aircraft Symposium of JSASS*, pp. 89-92, 1997(in Japanese).

[4] L. Ljung, " System Identification -Theory for the User (2nd edition)", Prentice Hall, Englewood Cliffs, NJ, 1999.

[5] J. C. Doyle, K. Glover, P. P. Khargonekar and B. A. Francis, " State-Space Solutions to Standard $\mathcal{H}_\infty$ and $\mathcal{H}_\in$ Control Problems", *IEEE Trans. on Automatic Control*, Vol. 34, No. 8, pp. 831-847, 1989.

[6] A. Tan, T. Kawada, A. Azuma, S. Saito and Y. Okuno, "Theoretical and Experimental Studies on System Identification of Helicopter Dynamics," *Proc. of 20th European Rotorcraft Forum-Amsterdam*, pp. 86.1-86.16, 1994.

[7] M. B. Tischler and M. G. Cauffman, "Frequency-Response Method for Rotorcraft System Identification," *Journal of the American Helicopter Society*, Vol. 37, No. 3, pp. 3-17, 1992.

[8] B. Etkin and L. D. Reid, "Dynamics of Flight (3rd edition)," John Wiley & Sons, Inc., 1995.